DNA: Not Merely the Secret of Life

The Origin and Development of Information-Directed Nanoscience

Nadrian C. Seeman

Department of Chemistry

New York University

New York, NY 10003, USA

ned.seeman@nyu.edu

I am delighted to receive the recognition of the Kavli Foundation, the Norwegian Academy of Science and Letters and the Norwegian Ministry of Education and Research for founding and developing structural DNA nanotechnology. This story begins about 50 years ago, when my Highland Park (IL) high school biology teacher, John Broming, devoted approximately the first 15% of his biology course to teaching his students elementary physics and chemistry, because he wanted us to recognize that biology is a physico-chemical phenomenon. From then on, I was fascinated with this point on the scientific spectrum at the Edge of Life, treating biology as a physical phenomenon. To focus a little more finely, I was particularly attracted by the fact that biology involved information and structure, not just disordered molecules tumbling around in solution. With this orientation, I chose to study biochemistry as an undergraduate student at the University of Chicago. Unfortunately, at that time and place, 'biochemistry' meant largely the study of the metabolic transformations of small molecules, which I found incredibly boring, a reaction reflected dramatically in my transcript. I was rescued from this combination of tedium and failure by the graduate student advisor, John Law, who sent me off to a biological crystallography graduate program in G.A. Jeffrey's crystallography department at the University of Pittsburgh. In Pittsburgh, Bryan Craven, Bob Rosenstein and Bob Stewart taught me about symmetry, 3D thinking, connected networks, and the electronic basis of matter, as well as how to solve crystal structures. I put this knowledge to good use when I was a postdoctoral fellow in Alexander Rich's laboratory at MIT, where my initial project was to solve the crystal structure of a dinucleoside phosphate that demonstrated the first high resolution image of the adenine-uracil base pairing proposed about 20 years earlier by Watson and Crick (Figure 1).[1] This success, convolved with Alex's infectious enthusiasm, hooked me on nucleic acids.

When I established my own laboratory at SUNY/Albany in 1977, I found to my dismay that, unlike my earlier experiences, people were not coming to me with difficult nucleic acid crystal structures for me to solve: I had to crystallize them myself! Crystallizing nucleic acid fragments (or anything else) is difficult, for good reason. Crystallization, particularly biological macromolecule crystallization, is arguably the least controllable experiment in modern science (Figure 2): You are trying to get an ensemble of molecules to line themselves up parallel to each other in a repeating arrangement in 3D by making them slowly insoluble in some solution. Often, you have no idea what intermolecular interactions you are trying to promote (hydrophobic? hydrophilic? ionic? a little of

each?). Typically, in a molecular crystal structure determination, you work out the molecular structure, and then, almost as an afterthought, you figure out what interactions are holding the crystal together. In addition, crystallization is a problem in a multidimensional conditions space, where, unlike most other experimental systems, it is impossible to optimize the individual parameters individually.

Thus, by September, 1980, at the start of the fourth year of my five-year probationary period as a faculty member, I had managed to crystallize nothing of interest to me or to anybody else; I was confronting a fatal progression that can be summarized as, "No crystals, no crystallography ... no crystallographer." What does a crystallographer do without crystals? The answer at the time was to write programs, one of the skills that came with the territory in the 1960s and 1970s. I was writing programs that simulated branch migration in the structures of 4-arm branched DNA molecules (called Holliday junctions), which are intermediates in genetic recombination. I was turned onto this study by Bruce Robinson, then a postdoc down the hall from me. Stimulated by an airplane conversation with Greg Petsko and a discussion with Kathy McDonough, then an undergraduate in my lab, I had figured out rules that permitted making synthetic branched junctions whose branch points would not migrate, unlike natural ones.[2] The rules I had worked out did not stop with 4-arm junctions, but also applied to junctions with more arms. One afternoon, I went over to the campus pub to have a beer and think about 6-arm junctions (Figure 3a). While sitting there alone, I suddenly thought of M.C. Escher's "Depth," (Figure 3b), and realized that the fish in that woodcut were topologically just like a 6-arm junction, with a head, a tail, a top fin, a bottom fin, a left fin and a right fin. For me the most important thing about the fish in "Depth" is that they are organized just like the molecules in a molecular crystal: The fish are parallel to each other, and repeat in a periodic array from front to back, from top to bottom, and from left to right.

I wondered if I could do that with branched nucleic acids. Escher was, of course, in control of all the features of his artwork. However, as a natural scientist, I needed a material interaction to control the contacts of DNA branched junctions. Fortunately, such an interaction was well-known in genetic engineering at the time, and it takes advantage of the information content of nucleic acids. The interaction is known as sticky-ended cohesion,[3] and it is the simple consequence of an overhang at the end of a DNA double helix (Figure 4a). If two overhangs are complementary, they will cohere with each other, just as two complementary DNA strands will pair with each other (Figure 4a). Sticky-ended

cohesion is thus an affinity interaction that can be programmed easily. There are, of course, many affinity interactions in biology, for example the interactions of antibodies and antigens. By contrast with the others, sticky-ended cohesion is unique: One cannot predict the 3D structure of any other affinity interaction without a crystal structure to provide the relevant details, but we know that the local structure of cohering sticky ends will be the traditional structure of DNA, known as B-DNA (Figure 4b).[4] Thus, we know how to program both the intermolecular affinity and the intermolecular structure of DNA species on a predictive basis. To my knowledge, this is a unique situation in structural chemistry, enabling the defined 3D self-assembly of well-defined stick-figures and networks (Figure 5).

By 1980, I had felt frustrated for several years with the analytical nature of crystallography, assuming that I was even lucky enough to obtain crystals. My success in demonstrating the structural details of A-U Watson-Crick base pairing had been a lucky punch, luckier than the numerous scientists who had preceded me during the previous years of A-U or A-T co-crystal structures that failed to show the sought-after base pairing. That story was followed by a structure even more difficult to solve, a complex of the same dinucleoside phosphate with the intercalating dye, 9-aminoacridine; that structure was an unlucky punch -- a lot of work, but the final structure did not demonstrate the structural features that we sought. Thus, the idea of designing my own crystals (not just hoping for the right interactions to prevail) was highly appealing to me.

Only two things stood in the way of my trying out this idea: I had no source of the synthetic DNA I needed, and I had no idea how to work with it in solution if I could get my hands on it. Although I learned to synthesize DNA (poorly) by hand, it took me five years to obtain a DNA synthesizing machine. In the meantime both these problems were solved by Neville Kallenbach: He bought DNA to test out early designs, and he taught me how to work with nucleic acids in solution. He also solved another very difficult problem for me: He rescued me from the biology department in Albany, where my research did not attract graduate students, and he offered me a position in the chemistry department at NYU, where my research was much more popular among the students.

The very first strands I made when I moved to New York in 1988 were the 10 strands Junghuei Chen used to make a DNA molecule whose edges were connected like the edges of a cube (Figure 6a). This construction signaled the start of structural DNA nanotechnology, but in fact we were only able to characterize the linking and branching topology of the molecule.[5] By that time we knew that

conventional branched junctions were somewhat floppy, so what we really knew we had made was a hexacatenane. A few years later, Yuwen Zhang built a 14-catenane, connected like the edges of a truncated octahedron (Figure 6b).[6] Both of these constructions were topological constructs, not really well characterized (or characterizable) geometrically.

Nevertheless, they fit in very well with another program within the lab, the construction of topological targets. It turns out that its double helical structure renders DNA almost the ideal topological synthetic component. This is evident from Figure 7a-7c, which shows that a half-turn of DNA corresponds to a crossing (a node), the fundamental unit that defines the topology of a knot or a catenane.[7] With this knowledge, John Mueller and Shouming Du built a variety of DNA knots (Figure 7d),[8,9] Hui Wang used an RNA knot to discover an RNA topoisomerase,[10] and Chengde Mao was able to attain the synthetic holy grail, Borromean rings (Figure 7e).[11]

It was very gratifying to get these topological results, but this direction would not lead to advances in *structural* DNA nanotechnology, because the products were inherently floppy. To build crystals, one needs rigid motifs, so that identical components cannot form cyclic assemblies which poison the growth of the periodic array. We devoted the middle 1990s to finding a rigid motif, and we found that the DNA double crossover (DX) structure was rigid enough for this purpose.[12] This molecule consists of two parallel helical domains joined twice by crossover structures formed between strands of opposite polarity. It seems possible to include as many parallel helices as desired in such structures. Xiaoping Yang built a robust 1D array from DNA triangles with a DX edge,[13] and together with Erik Winfree, Furong Liu and Lisa Wenzler, we built a 2D crystal from DX molecules.[14] You can include an extra double helical domain (perpendicular to the plane of the helix axes) on some of these molecules, so it was possible to build a striped pattern with designed dimensions (Figure 8).

The advent of a robust motif enabled not only 2D structures, but also the first DNA-based nanomechanical devices. The original notion to build a DNA nanomechanical device based on the B-Z transition (reflecting a shift from right-handed DNA to left-handed DNA) had come in 1987. Demonstrating it was another matter. It required a stable shape that could be changed when the device changed state; the most reliable way to do the demonstration was to produce a change in a FRET signal. However, a floppy motif could not yield this change, only a robust motif could do it. After a number of false starts, Chengde Mao was able to provide this demonstration about a dozen years after the machine

had first been conceived (Figure 9a).[15]

The key problem with the B-Z device is its lack of individual addressability, because it is most readily formed with sequences of $(CG)_n$. Thus, even if many of the components of the device were to be changed, there would still be (except for some chemical nuance), only two states, the B-state and the Z-state, because the state is a function of the environment, rather than a specific triggering agent that targets a particular molecule. We solved this problem by devising the PX-JX_2 device, which was brought to fruition by Hao Yan.[16] PX and JX_2 are two robust DNA motifs that differ from each other by a half-turn rotation of one end relative to the other (Figure 9b). They can be interconverted if the strands that comprise them are divided into a control region (which can be varied) and a frame region. These control elements can be switched from strands directing the system into the PX state to strands directing the system into the JX_2 state. The control strands that direct the system into one state can be removed by using a 'toehold,' an unpaired extension to the strand; the full complement to the strand (including the toehold) will bind the toehold and then branch migrate through the rest of the strand; this method was developed by Bernard Yurke and his colleagues.[17] The use of the toeholds in the machine cycle of the PX-JX_2 device is shown in Figure 9b; Figure 9c shows that the motions of the device can be seen in the AFM. The toehold-strand removal process relies on the notion that there are more base pairs formed after a given strand or set of strands is added to solution than there were before, providing a thermodynamic driving force for the change of state. Another type of system, based on the same principle, is the walker, which moves on a sidewalk. Bill Sherman developed a walker that moved according this type of driving force.[18] However, every time a change of state was needed, one had to add the appropriate strand to remove an anchoring strand from the sidewalk, and then one had to add the next strand. About five years later, Tosan Omabegho built an autonomous walker that used fuel strands in solution in a cascade system that drove a walker forward by several steps.[19]

Having made both a robust sequence-dependent device and two-dimensional lattices, it was a natural goal to combine them, so that the devices could be embedded into a lattice. This was done by Baoquan Ding, who developed a cassette to anchor the device in a 2D-array. In addition to the PX-JX_2 device and a domain to anchor the cassette in a DNA array, the cassette also contained a small robot-arm. The direction of this arm could be switched while the cassette was embedded in the 2D array, so the two advances were successfully combined in this system.[20] So as to demonstrate the motion, it was

necessary to make eight different tiles and self-assemble a lattice with eight molecules per repeat (Figure 10). The generation of large addressable arrays was greatly simplified by Paul Rothemund's 2006 development of DNA origami: By using a 7500 nucleotide viral single-strand, he was able to self-assemble a two-dimensional array with an addressable surface area roughly three times that of the eight-tile array.[21] From then on, we used DNA origami when we needed large addressable surfaces.

The individual addressability of the PX-JX_2 device has been demonstrated in several different projects. Shiping Liao used it to make a device that translated DNA sequences into polymer assembly instructions.[22] This work was followed by further progress in individual addressability from Hongzhou Gu and Jie Chao, who were able to anchor a pair of PX-JX_2 cassettes in a DNA origami array.[23] The two cassettes faced each other, and each contained a sticky end. When the state of a cassette was changed, then the sticky ends would switch their order. In all, four different states for the tile could be obtained. The four different states were used to capture four different tiles, which could be identified using the AFM. The most exciting use of individual addressability so far is the recent development of a nanoscale assembly line, also built by Hongzhou Gu and Jie Chao.[24] This combination of components uses a DNA origami array as its base, in which three different cassettes are anchored. Each of these cassettes carries different configurations of nanoparticle cargoes. The origami also contains a track for a three-fold-symmetric walker. As the walker walks past each of the cassettes, the state of the cassette (PX or JX_2) controls whether a particular cargo is loaded onto the walker (Figure 11). With three different 2-state devices, one can assemble eight different products, depending on the programming of the system. It is straightforward to use a transmission microscope to demonstrate that these eight products can be prepared using the assembly line.

I have left the crystal story hanging, as I went off on a tangent about the consequences of robust motifs for nanomechanical devices. However, we certainly never forgot that our key goal was to control the structure of matter in 3D, to the highest extent possible. Harking back to Escher's fish, this meant getting a robust DNA motif to self-assemble into designed macroscopic 3D crystals. When you move from 2D to 3D, the standards for success go up. In 2D, molecules are typically characterized by atomic force microscopy. With the types of samples we have, this means that our resolution is around 5-10 nm. However, when you move from 2D to 3D, the methodology changes as well, and you use X-ray crystallography for characterization. Crystallography can reveal structures to resolutions of 1 Å or

better, and the quality of a crystal structure determination is usually limited by the quality of the sample, rather than by the measuring apparatus. Thus, not only do crystals have to be relatively large (~200 microns in each direction is good), but they also have to be very well ordered. We were very pleased when we were able to take the tensegrity-triangle motif, originated in Chengde Mao's laboratory,[25] and get it to give us crystals that diffracted to 4 Å resolution.[26] In addition to Chengde and his student Yi Chen, the effort in my lab was led by Jianping Zheng, Jens Birktoft, Tong Wang, Ruojie Sha and Pam Constantinou, while Steve Ginnell and Bob Sweet were enormously helpful with the data collection. The structure of the individual molecule is shown stereoscopically in Figure 12a, and the way two molecules are held together by a sticky end is shown n Figure 12b. The tensegrity-triangle motif spans 3-space, a point emphasized by the stereoscopic image in Figure 13a, which shows the environment of each triangle. The unit cell consists of a rhombohedron, and the rhombohedral cavity is seen dramatically in a stereoscopic projection in Figure 13b.

The key point behind this self-assembly is that we did not just land a lucky punch. There are at least eight more variations on this theme, all designed to self-assemble on the same basis as the system shown in Figures 12 and 13. These crystals include asymmetric versions of the triangle shown above, and other versions with edges containing three and four turns. Tong Wang also deliberately crystallized the molecule with two repeats per asymmetric unit. In an interesting variation on this theme, leading to our goal of the crystals acting as hosts, has been done by Ruojie Sha. Ruojie has covalently attached a red dye (Cy3) to one of the unique molecules, or to both. Likewise, he has attached a blue dye (Cy5) to one or both of the unique molecules. There are nine combinations (including no attachment), and he has produced crystals colored as designed, Cy3 and no Cy5 is red; Cy5 and no Cy3 is blue, and one on each molecule is purple (Figure 14).

We have done a lot more experiments over they years, and I have neglected to mention many people who contributed to our efforts. The point of this article is to show the progress made, largely in our laboratory, towards the goals we enunciated thirty years ago. However, the most important thing that has happened to structural DNA nanotechnology is that it has not remained the preoccupation of a single laboratory. It has grown to the extent that at least 60 laboratories have participated in the field, and the sixty fertile minds directing the talented students and postdocs engaged in those efforts are taking the field far beyond what could ever be done in a single lab. The field is now an active

participant in the design of the next generations of therapies, computation, nanoelectronics and, nanophotonics, as well as probing the contents of the living cell. Our species' history could easily be written as the history of its control of materials and the ways that it has used them in furthering its goals. It is clear that this generation's use of the information inherent in DNA-based materials and machines will contribute to significant progress in that direction.

ACKNOWLEDGEMENTS

I thank all of my students, postdocs, collaborators and colleagues, who brought this field to its current state. This research has been supported by grants GM-29544 from the National Institute of General Medical Sciences, CTS-0608889 and CCF-0726378 from the National Science Foundation, 48681-EL and W911NF-07-1-0439 from the Army Research Office, N000140910181 and N000140911118 from the Office of Naval Research and a grant from the W.M. Keck Foundation.

REFERENCES

1. N.C. Seeman, J.M Rosenberg, F.L. Suddath, J.-J.P. Kim and A. Rich, RNA Double Helical Fragments at Atomic Resolution I: The Crystal and Molecular Structure of Adenylyl-3',5'-uridine Hexahydrate. *J. Mol. Biol.* **104**, 109-144 (1976).
2. N.C. Seeman, Nucleic Acid Junctions and Lattices. *J. Theor. Biol.* **99**, 237-247 (1982).
3. S.N. Cohen, A.C.Y. Chang, H.W. Boyer, R.B. Helling, Construction of biologically functional bacterial plasmids *in vitro*, *Proc. Nat. Acad. Sci. (USA)* **70**, 3240-3244 (1973).
4. H. Qiu, J.C. Dewan and N.C. Seeman, A DNA Decamer with a Sticky End: The Crystal Structure of d-CGACGATCGT. *J. Mol. Biol.* **267**, 881-898 (1997).
5. J. Chen and N.C. Seeman, The Synthesis from DNA of a Molecule with the Connectivity of a Cube, *Nature* **350**, 631-633 (1991).
6. Y. Zhang and N.C. Seeman, The Construction of a DNA Truncated Octahedron, *Journal of the American Chemical Society* **116**, 1661-1669 (1994).
7. N.C. Seeman, The Design of Single-Stranded Nucleic Acid Knots, *Molec. Eng.* **2**, 297-307 (1992).
8. J.E. Mueller, S. M. Du and N.C. Seeman, The Design and Synthesis of a Knot from Single-Stranded DNA, *J. Am. Chem. Soc.* **113**, 6306-6308 (1991).
9. S.M. Du, B.D. Stollar, and N.C. Seeman, A Synthetic DNA Molecule in Three Knotted Topologies, *J. Am. Chem. Soc.* **117**, 1194-1200 (1995).
10. H. Wang, R.J. Di Gate, and N.C. Seeman, An RNA Topoisomerase, *Proc. Nat. Acad. Sci. (USA)* **93**, 9477-9482 (1996).

11. C. Mao, W. Sun and N.C. Seeman, Assembly of Borromean Rings from DNA, *Nature* **386**, 137-138 (1997).
12. X. Li, X. Yang, J. Qi, and N.C. Seeman, Antiparallel DNA Double Crossover Molecules as Components for Nanoconstruction, *J. Am. Chem. Soc.* **118**, 6131-6140 (1996).
13. X. Yang, L.A. Wenzler, J. Qi, X. Li and N.C. Seeman, Ligation of DNA Triangles Containing Double Crossover Molecules, *J. Am. Chem. Soc.* **120**, 9779-9786 (1998).
14. E. Winfree, F. Liu, L. A. Wenzler, and N.C. Seeman, Design and Self-Assembly of Two-Dimensional DNA Crystals, *Nature* **394**, 539-544 (1998).
15. C. Mao, W. Sun, Z. Shen and N.C. Seeman, A DNA Nanomechanical Device Based on the B-Z Transition, *Nature* **397**, 144-146 (1999).
16. H. Yan, X. Zhang, Z. Shen and N.C. Seeman, A Robust DNA Mechanical Device Controlled by Hybridization Topology, *Nature* **415**, 62-65 (2002).
17. B. Yurke, A.J. Turberfield, A.P. Mills, Jr., F.C. Simmel and J.L. Newmann, A DNA-Fuelled Molecular Machine Made of DNA, *Nature* **406**, 605-608 (2000).
18. W.B. Sherman and N.C. Seeman, A Precisely Controlled DNA Bipedal Walking Device, *NanoLetters* **4**, 1203-1207 (2004).
19. T. Omabegho, R. Sha and N.C. Seeman, A Bipedal DNA Brownian Motor with Coordinated Legs, *Science* **324**, 67-71 (2009).
20. B. Ding and N.C. Seeman, Operation of a DNA Robot Arm Inserted Into a 2D DNA Crystalline Substrate, *Science* **314**, 1583-1585 (2006).
21. P.W.K. Rothemund, Scaffolded DNA Origami for Nanoscale Shapes and Patterns. *Nature* **440**, 297-302 (2006).
22. S. Liao and N.C. Seeman, Translation of DNA Signals into Polymer Assembly Instructions, *Science* **306**, 2072-2074 (2004).
23. H. Gu, J. Chao, S.J. Xiao and N.C. Seeman, Dynamic Patterning Programmed by DNA Tiles Captured on a DNA Origami Substrate, *Nature Nanotech.* **4**, 245-249 (2009).
24. H. Gu, J. Chao, S.J. Xiao & N.C. Seeman, A Proximity-Based Programmable DNA Nanoscale Assembly Line, *Nature* **465**, 202-205 (2010).
25. D. Liu, W. Wang, Z. Deng, R. Walulu and C. Mao, Tensegrity: Construction of Rigid DNA

Triangles with Flexible Four-Arm Junctions, *J. Am. Chem. Soc.* **126**, 2324-2325 (2004).

26. J. Zheng, J.J. Birktoft, Y. Chen, T. Wang, R. Sha, P.E. Constantinou, S.L. Ginell, C. Mao, and N.C. Seeman, From Molecular to Macroscopic *via* the Rational Design of a Self-Assembled 3D DNA Crystal, *Nature* **461**, 74-77 (2009).

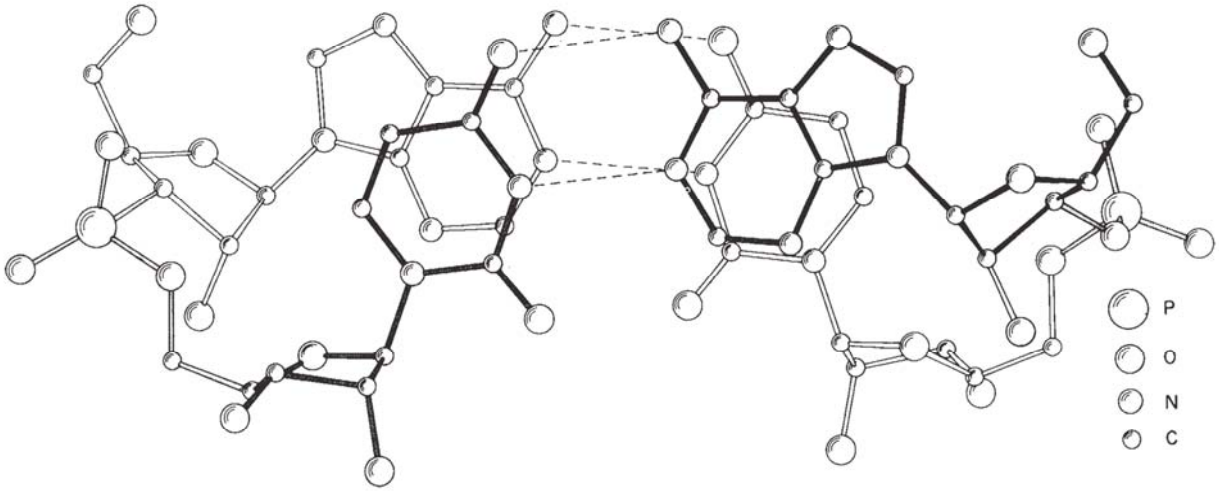

Figure 1. *The Crystal Structure of the Dinucleoside Phosphate ApU.* The two hydrogen bonds that produce the A-U base pairing is seen readily in this view.

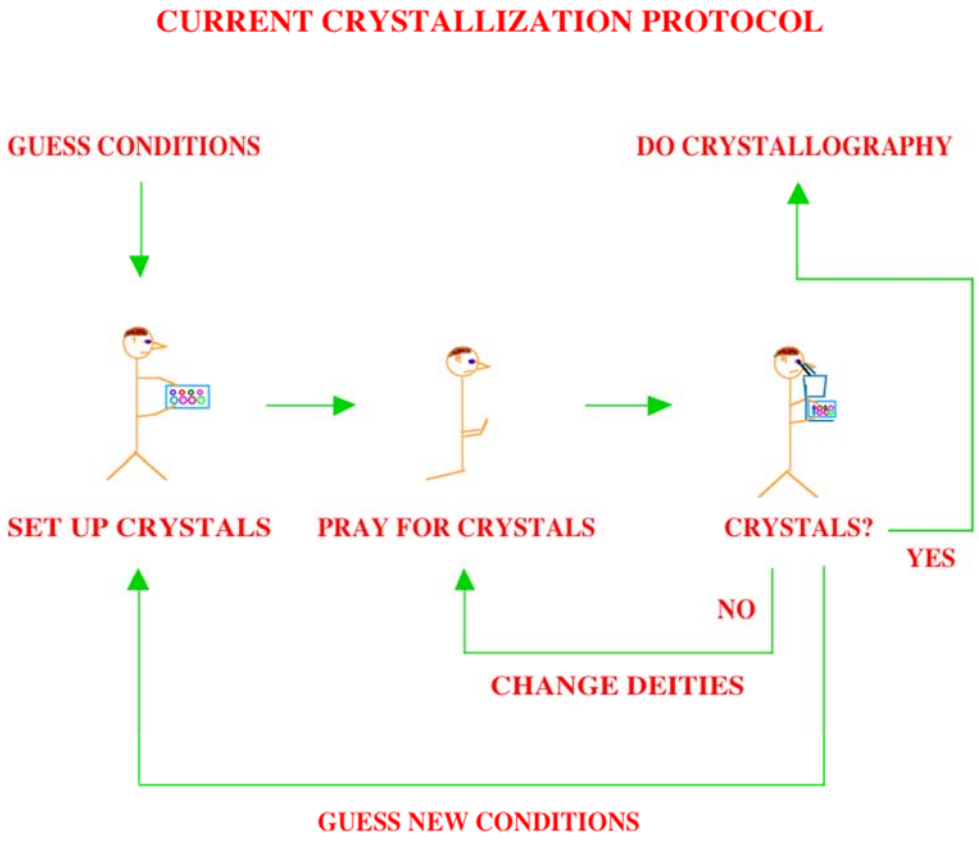

Figure 2. *The Crystallization Protocol Usually Used to Produce Macromolecular Crystals.* The most difficult aspect of this procedure is that failure gives few if any hints as to ways to correct the errors, so as to achieve success on the next round.

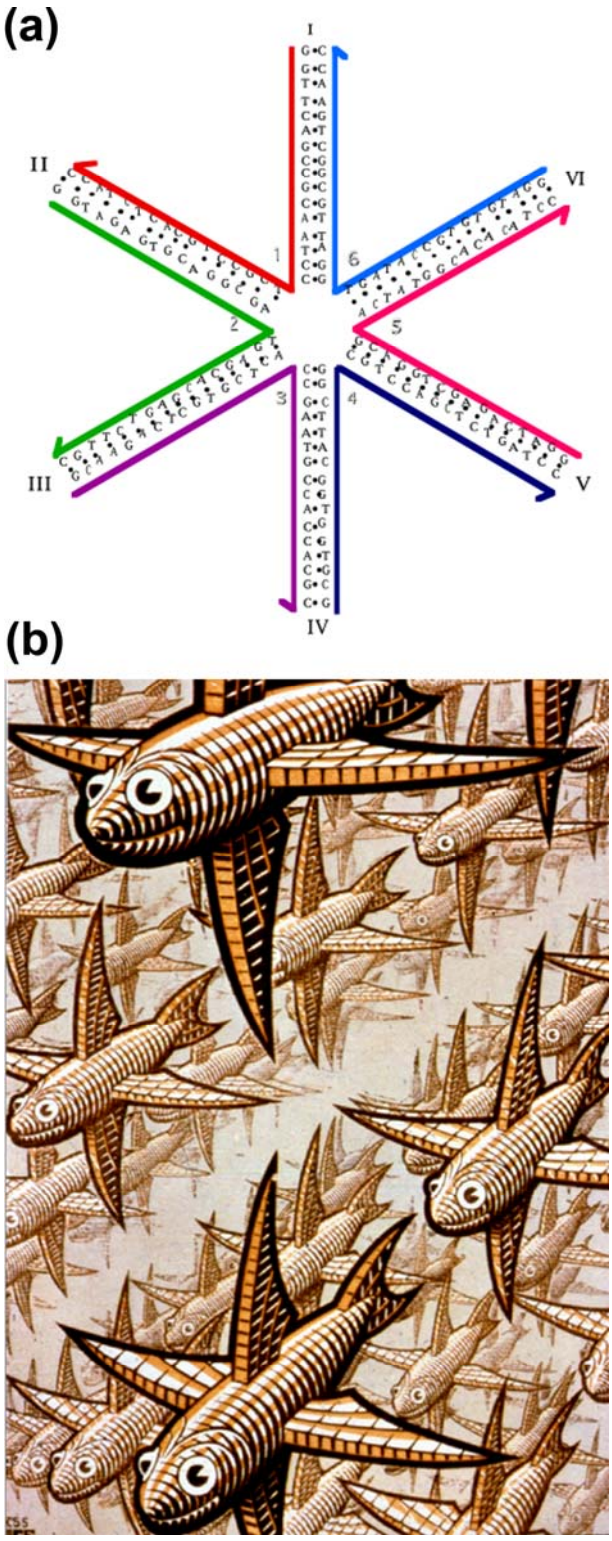

Figure 3. *The Inspiration for Information-Based Nanoscience.* The six-arm junction seen in panel *(a)* is similar to the fish in Escher's woodcut 'Depth'. Both have six features emanating from their centers. The 6-arm junction has six different arms flanking its center. In the case of the fish, there is a head, a tail, a top fin, a bottom fin, a left fin and a right fin. It is key that the fish are arranged like the molecules in a molecular crystal, with periodicity front to back, top to bottom and left to right. The central notion was that perhaps branched DNA could be organized similarly.

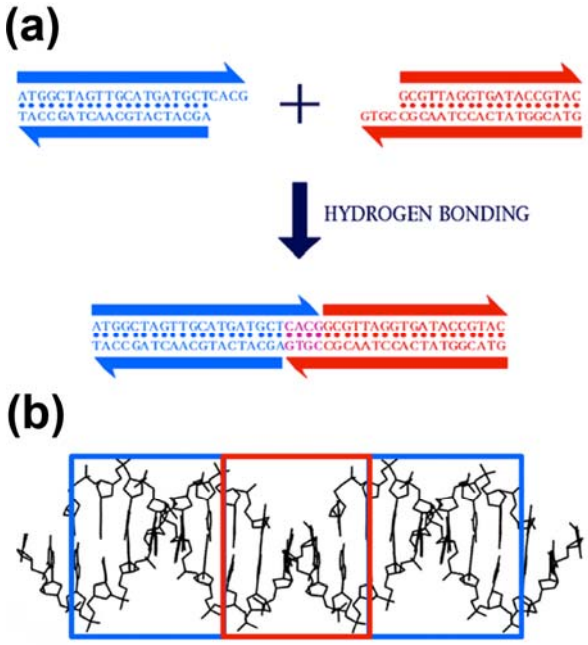

Figure 4. *Sticky-Ended Cohesion.* Panel *(a)* shows in schematic form how two DNA molecules containing complementary overhangs can cohere through hydrogen bonding to produce a single molecular construct. Panel *(b)* shows a crystal structure[4] held together in one direction by sticky ends. The two-nucleotide sticky ends are visible in the red box. Their structure is the same (except for being upside down, because they are a half-turn away) as the comparable regions in the blue boxes. Consequently, sticky ends are an interaction whereby both the partners can be programmed, and their 3D structures are known on a predictive basis.

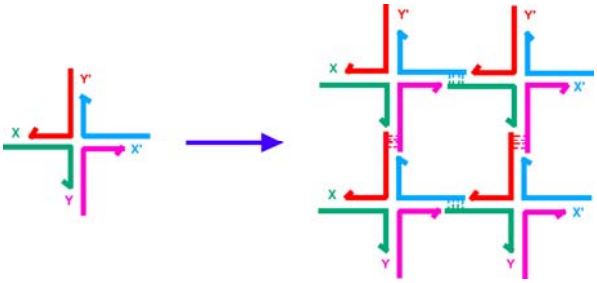

Figure 5. *Self-assembly of Branched DNA.* The 4-arm branched DNA molecule on the left is tailed by complementary sticky ends X and X', as well as Y and Y'. On the right, they cohere to form a quadrilateral. Further sticky ends are available on the outside of the quadrilateral to continue self-assembly to form a lattice.

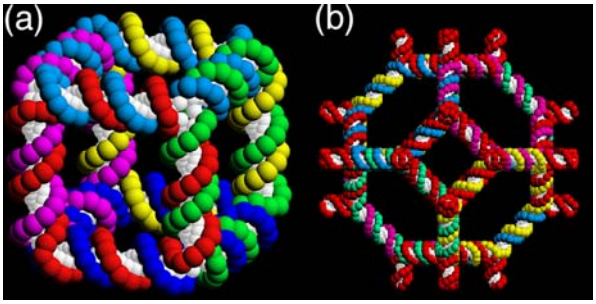

Figure 6. *Two Early Constructs from DNA Nanotechnology*. The molecule on the left has the connectivity of a cube and the one on the right has the connectivity of a truncated octahedron. The vertices correspond to branch points in DNA branched junctions, and the edges consist of DNA double helices. Both molecules contain two turns per edge, so that they are catenanes in which each face corresponds to a single strand linked twice to the strands that flank it; the cube is hexacatenane and the truncated octahedron is a 14-catenane. The shapes are idealizations.

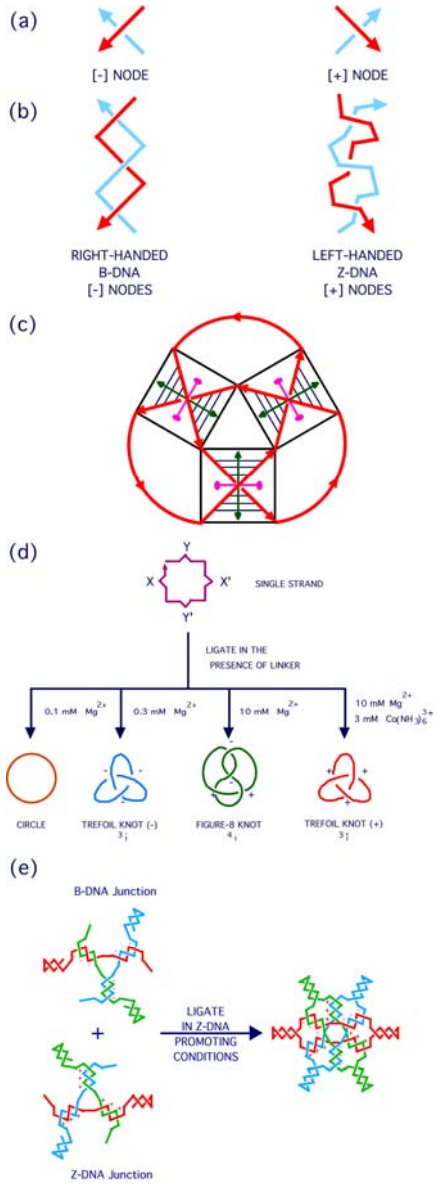

Figure 7. *Topological Constructs.* Panel *(a)* shows the mirror relationship between negative nodes and positive nodes. Panel *(b)* shows schematically that conventional right-handed B-DNA forms negative nodes and that left-handed Z-DNA forms positive nodes. Panel *(c)* shows a trefoil knot produced by three half-turns of B-DNA. Panel *(d)* shows how a linear strand containing two complementary single-turn stretches, one labeled X and X' and the other labeled Y and Y' can produce different knots depending on the conditions under which it is sealed to form a closed arc. The X duplex has a different propensity to form left-handed Z-DNA than the Y duplex. Consequently, increasing the ionic strength of the system can yield the circle, the trefoil knot with all negative nodes, the figure-8 knot (two positive and two negative nodes) and the trefoil knot with all positive nodes. Panel *(e)* shows how ligating two 3-arm junctions, one in the B-state and the other in the Z-state, leads to Borromean rings.

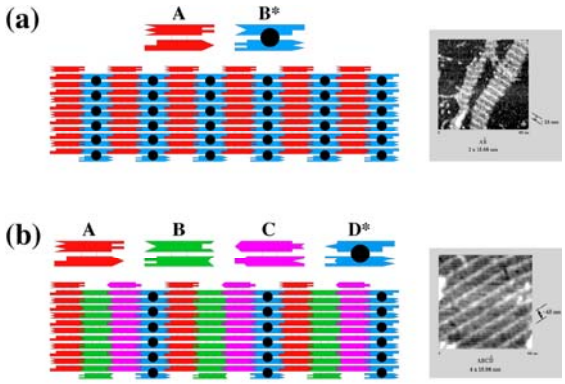

Figure 8. *The Formation of 2D Arrays from DX Tiles.* Panel *(a)* shows a schematic of two tiles, a red one (A) and a blue one (B). The complementary nature of their sticky ends is shown geometrically. The B-tile contains another domain (the black dot) that is oriented perpendicular to the plane of the array. This feature leads to stripes in the AFM image. The width of the tiles is 16 nm, so this array should produce stripes separated by ~32 nm, which is seen in the AFM image to the right of the schematic. Panel *(b)* shows four tiles of the same dimension, only one of which contains the stripe-producing feature. This leads to stripes separated by ~64 nm, as seen in the AFM to the right.

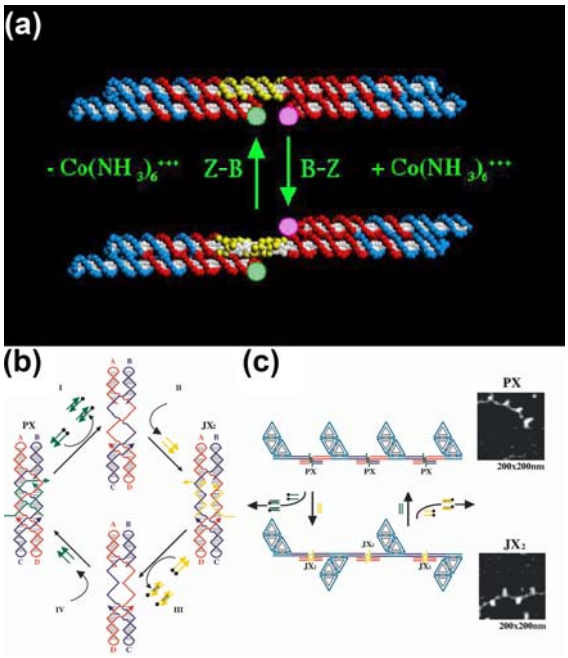

Figure 9. *DNA-Based Nanomechanical Devices.* Panel *(a)* illustrates a device based on the B-Z transition of DNA. Two DX molecules are connected by a shaft of yellow nucleotide pairs with a sequence that enables them to undergo the transition from right handed B-DNA to left-handed Z-DNA under the right solution conditions. The addition of $Co(NH_3)_6^{3+}$ provides conditions favorable to the transition, and results in the bottom domain on the right rotating to the top of the long double helix. The transition is monitored by fluorescence resonance energy transfer (FRET) between dyes represented by the green and pink circles inthe diagram. Panel *(b)* illustrates the machine cycle of the sequence-dependent PX-JX_2 device. Starting on the left, the system is in the PX state. Removal of its green set strands (process I) produces a naked frame. Addition of yellow set strands (Process II) produces the JX_2 state. Note that the relative rotations of the top and bottom pairs of helices are switched in the two states. The state can be reversed by removing the yellow set strands (Process III) and adding the green set strands (Process IV). Panel *(c)* This illustrates image shows that the state of the system can be visualized in the AFM. The device is used to connect a series of half-hexagonal DNA trapezoids. When in the PX state, the array is parallel, but it assumes a zig-zag arrangement in the JX_2 state.

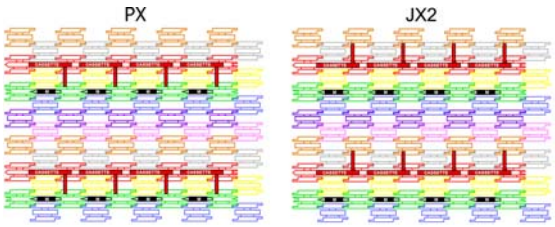

Figure 10. *The Motion of a Robot Arm in a 2D DNA Tile Array.* A cassette has been developed that incorporates the PX-JX_2 device into an array consisting of eight unique tiles (note the eight colors), each containing three domains of DNA. The cassette contains a robot arm that points in one direction or the other, depending on the state of the device. This is visible in the image, where it points towards a black marker in the PX state and it points away from the black marker in the JX_2 state. Both the cassette and the marker have been rephased by three nucleotide units, so they are roughly perpendicular to the plane of the array.

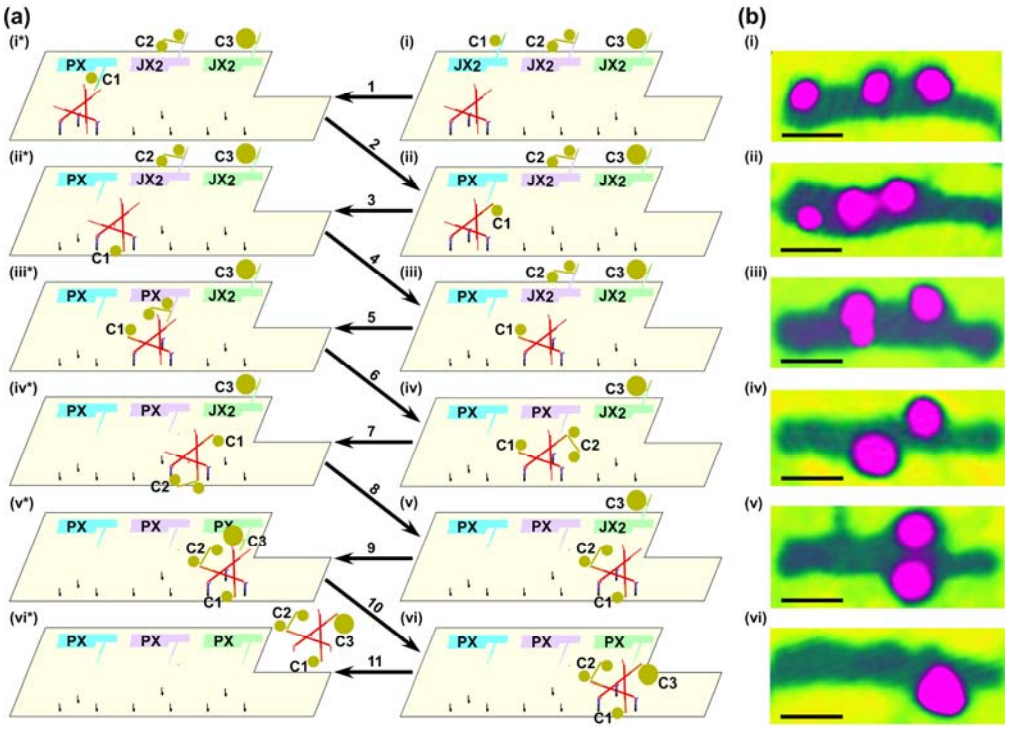

Figure 11. *The Operation of a Nanoscale Assembly Line.* Schematics are shown in (a) and atomic force micrographs of the right column of (a) are shown in (b). AFM was performed by tapping in air; this mode of AFM results in only the nanoparticles and the origami being visible, and the individual nanoparticle components are not resolved from each other. Owing to the washing procedures between steps, the AFM images are not of the same individual assembly line. Panel i illustrates the origami array with cassettes and walker in the starting position. The cassettes are set to the default JX_2 state, with the arms pointing away from the walker pathway. Different cargoes on the arms (5 nm Au on cassette 1, a linked 5 nm Au pair on cassette 2, and a 10 nm Au on cassette 3) are visible both schematically (a) and in the AFM (b). Step 1 shows cassette 1 switched from the JX_2 state to the PX state, bringing cargo 1 close to the walker hand. Step 2 illustrates the addition of cargo 1 from the cassette 1 to the walker by DNA branch migration; the movement of cargo 1 is evident in the AFM (ii). Step 3 shows the walker with cargo 1 walking the 1st step along the pathway; step 4 illustrates the walker with cargo 1 walking the 2nd step, positioning itself near cassette 2, which is visible both schematically and in the AFM (iii). Step 5 shows cassette 2 is switched from the JX_2 state to the PX state, bringing cargo 2 close to the walker. Step 6 illustrates the addition of cargo 2 from cassette 2 to the walker by branch migration; the addition of cargo 2 is evident in the AFM (iv). Step 7 shows the walker with cargo-1 and cargo-2 walking the 3rd step along the pathway. Step 8 illustrates the walker with both cargo 1 and cargo 2 walking the 4th step to be close to cassette 3; the walking is clearly visible in the AFM (v). Step 9 shows cassette 3 switched from the JX_2 state to the PX state, bringing cargo 3 close to the walker. Step 10 illustrates the addition of cargo 3 from cassette 3 to the walker by branch migration; the addition of cargo 3 is visible in the AFM (vi). Step 11 shows the walker with all three cargo components released from the origami. By separately programming the device, eight different products can be produced. All scale bars are 50 nm.

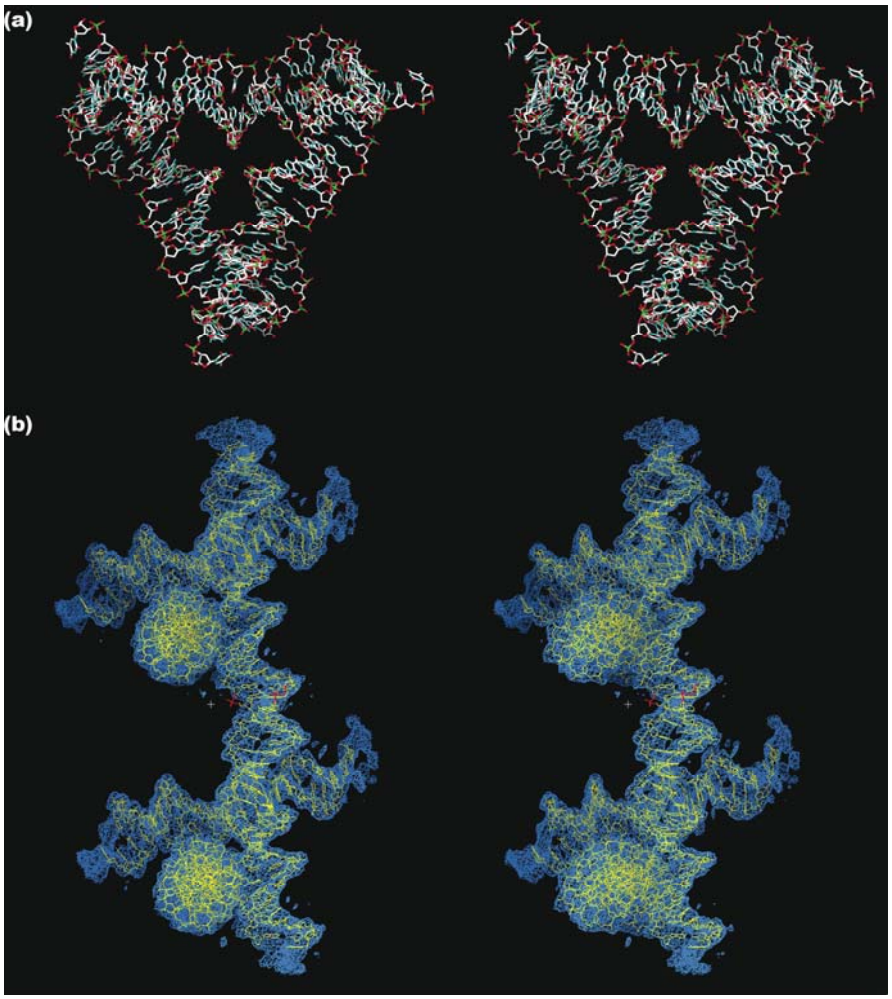

Figure 12. *Stereoscopic Representation of the Contents of a Designed Self-Assembled DNA Crystal.* Panel *(a)* shows a molecular drawing of the basic tensegrity triangle that is the repeating element of the crystalline array. Panel *(b)* shows how tow of the triangles are connected by sticky ends.

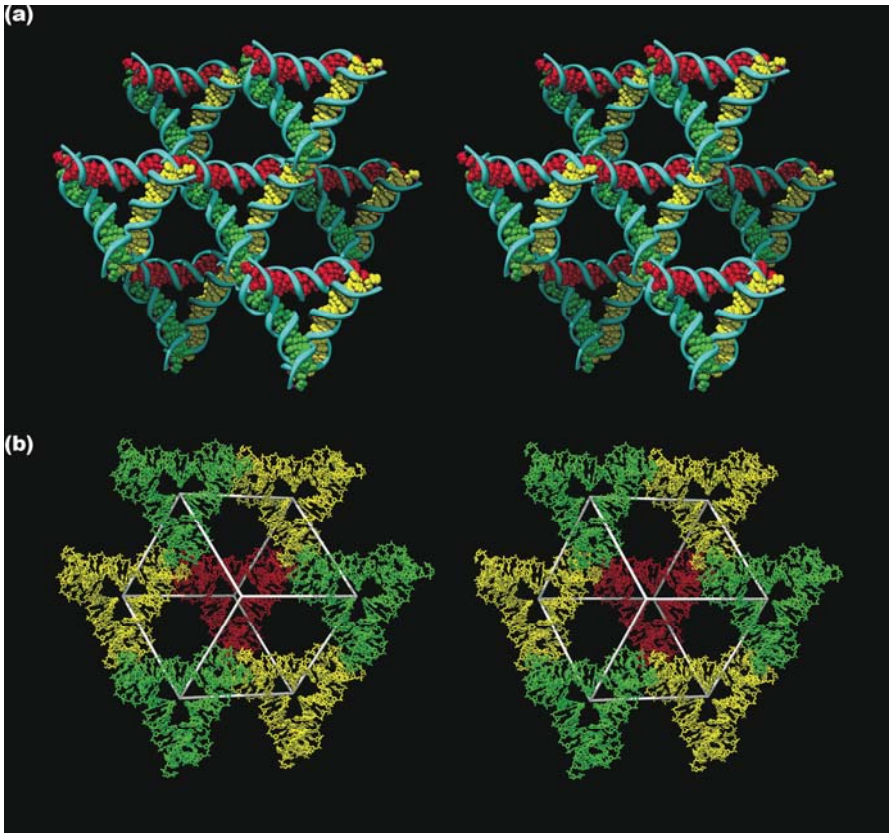

Figure 13. *The Lattice Formed by the Tensegrity Triangles. (a) The Surroundings of an Individual Triangle.* This stereoscopic simplified image distinguishes the three independent directions by the colors (red, green and yellow) of their base pairs. Thus, the central triangle is shown flanked by three other pairs of triangles in the three differently colored directions. *(b) The Rhombohedral Cavity Formed by the Tensegrity Triangles.* This stereoscopic projection shows seven of the eight tensegrity triangles that comprise the corners of the rhombohedron. The outline of the cavity is shown in white. The red triangle at the back connects through one edge each to the three yellow triangles that lie in a plane somewhat closer to the viewer. The yellow triangles are connected through two edges each to two different green triangles that are in a plane even nearer the viewer. A final triangle that would cap the structure has been omitted for clarity. This triangle would be directly above the red triangle, and would be even closer to the viewer than the green triangles.

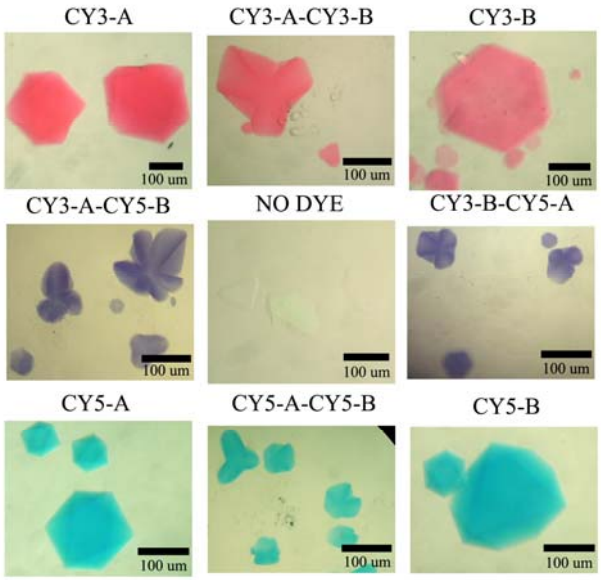

Figure 14. *Control of Crystal Color by Attachment of Dyes to Different Molecules within the Crystallographic Repeat.* The two independent molecules in the crystallographic repeat are designated as A and B. Two dyes are used, CY3, which is a pink dye, and CY5, which is a blue dye. The central panel is a control with no dyes attached to either molecule. The top row shows the three combinations of attaching CY3 to the different molecules, with the result that all are pink. The bottom row shows the same attachment series for CY5, yielding all blue crystals. The two side panels in the middle row show that combining the dyes in either order leads to purple crystal.